Quantifying Energy Balance across Different Biomes Using Remotely Sensed Data

Rehel A. Diaz[1], Jose Edwin C. Cubelo[1], Arsenio D. Bulfa Jr.[1], Kezia Shem G. Brusola[2]

[1]College of Agriculture, Silliman University, Dumaguete City 6200, Philippines; [2]Institute of Agricultural and Biosystems Engineering, College of Engineering and Agro-Industrial Technology, UPLB, College, 4030 Laguna, Philippines.

Abstract

Although there are existing remotely-sensed data that directly calculate the surface energy balance parameters, their spatial resolution is low. With this, a method called Simplified Surface Energy Balance Index was used to estimate energy balance components. From the different remotely-sensed data, downscaled maps of net radiation, latent, sensible, and ground heat fluxes were generated for the province of Laguna. The values of these parameters were measured for water, urban, forest, and agricultural areas. It was found that latent heat flux was highest for all the biomes while soil heat flux was the lowest. Comparing the components for each biome, latent heat flux was high in forest and water bodies due to the availability of water, which is a factor of evaporation. On the other hand, ground heat flux and sensible heat flux were high in urban and agricultural areas, both representing dry areas. Overall, net radiation is inversely proportional to reflectance. Water had low albedo, therefore high net radiation. The urban and agricultural areas had high albedo, which indicates low net radiation. The method employed in this study is helpful to estimate the partitioning of the surface energy balance parameters, especially in the absence of instruments that directly measure them.

Keywords: Energy Balance, Biomes, Remotely sensed data

Introduction

Surface energy balance is the partitioning of net radiation into sensible heat, latent heat, and ground heat. Caused by a change in temperature, sensible heat flux is the heat energy transferred between the surface and air when there is a temperature gradient between the surface and the air above. Meanwhile, latent heat flux is the quantity of heat absorbed or released by water undergoing phase change at constant air temperature and pressure. Lastly, ground heat flux is due to heat conduction of the soil (Odhiambo & Irmak 2015).

The components and partitioning of surface energy balance greatly depend on the surface covers, moisture, temperature, wind, and other micrometeorological parameters. During the daytime on a moist surface, the partition of net radiation is dominated by latent heat. There is also a moderately sensible flux and a very low and negligible soil heat flux. On the dry surface, in contrast, the partition of net radiation during daytime is dominated by sensible heat. Soil heat flux is also high in dry surface conditions but almost no or zero latent heat flux. There is an observable variation in the quantity of each component of the surface energy balance across different ecosystems. In a well-watered vegetated surface, for instance, latent heat accounts for 60% of the net radiation, while sensible heat flux constitutes 28% of the net radiation. Soil heat flux in this ecosystem is only 12% of the net radiation. In the desert, on the other hand, latent heat flux is almost zero, and sensible heat flux accounts for a huge percentage of the net radiation. Ground heat flux in this condition is also high. There are also instances or conditions where some of the partitions of the surface energy balance become higher than the net radiation. In a well-irrigated herbaceous crop on a sunny day in an oasis that is surrounded by a large expanse of desert, for example, an abundant supply of water and advection makes latent heat flux higher than the net radiation (Saludes, 2018).

Simplified Surface Energy Balance Index (S-SEBI) is a method of estimating latent and sensible heat. It is dependent on remotelysensed data specifically albedo and minimum and maximum surface temperature. Typically, the surface temperature is low at a lower reflectance level but as it enters the evaporation-

controlled portion, the temperature begins to increase with albedo. Due to heating in this state, there is a decrease in evaporation which results in a decrease in water availability. In another portion called radiation-controlled, as albedo increases, the surface temperature begins to decrease. It is where evaporation will not happen and the remaining energy is used for surface heating (Liou & Kar, 2014). Figure 1 shows the plot of surface temperature and albedo (Roelink et al., 1999).

Figure 1

Surface Reflectance vs Surface Temperature Using S-SEBI Model

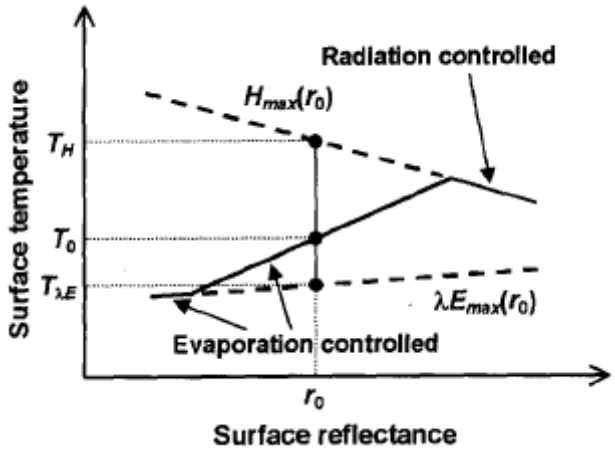

Remote sensing is an innovation to analyze an area spatially and temporally using satellite images. It is widely used in urban planning, forestry, biodiversity, weather, and agriculture. Google Earth Engine (GEE) is an online GIS that stores satellite imagery in an archive accessible to its users. It uses JavaScript API so that one can analyze the data of a specific area (GEE, 2018).NDVI measuresthe greenness and photosynthetic capacity of the vegetation. NDVI algorithm takes advantage of the fact that green vegetation reflects less visible light and more NIR, while sparse or less green vegetation reflects a greater portion of the visible and less nearIR. NDVI combines these reflectance characteristics in a ratio so it is an index related to photosynthetic capacity. Plant photosynthetic activity is determined by chlorophyll content (Verhulst & Govaerts, 2010*).*

The range of values obtained is between −1 and +1. Only positive values correspond to vegetated; the higher the index, the NDVI measures the greenness and photosynthetic capacity of the vegetation. NDVI algorithm takes advantage of the fact that green vegetation reflects less visible light and more NIR, while sparse or less green vegetation reflects a greater portion of the visible and less nearIR. NDVI combines these reflectance characteristics in a ratio so it is an index related to photosynthetic capacity. Plant photosynthetic activity is determined by chlorophyll content (Verhulst and Govaerts 2010). The range of values obtained is between −1 and +1. Only positive values correspond to vegetated zones; the higher the index, the greater the chlorophyll content of an area. The time of maximum NDVI corresponds to the time of maximum photosynthesis. Seasonally integrated NDVI indicates photosynthetic activity during the growing season. The rate of change in NDVI may indicate the speed of increase or decrease of photosynthesis. Changes in vegetation cover directly impact surface water and energy budgets through plant transpiration, surface albedo, emissivity, and a roughness according to Aman et al. (1992, as cited in Jiang et al., 2006).

Laguna is a province located in the north-central part of Region IV-A or CALABARZON. It has an area of 191,785 hectares. It is situated near two dormant volcanoes namely Mount Makiling and Mount Banahaw. Also, the province encloses Laguna de Bay which is the largest freshwater lake in the country (LLDA, 2018). A number of the population in Laguna are engaged in agriculture producing rice, coconut, sugarcane, lanzones, and other citrus fruits (PhilGIS, 2018). According to climate classification based on average monthly rainfall in the Philippines, devised by Fr. J. Corona, Laguna has a Type I climate that has two pronounced seasons: dry from November to April and wet during the rest of the year (Lantican, 2001). Over the years, remote sensing methods have been utilized and improved following the advancement in satellite technology and computing power. With these innovations, fewer ground-based measurements of model parameters are required, and models can be applied more accurately over larger extents at higher spatiotemporal resolution (McShane et al., 2017).

Quantifying energy balance is useful in agriculture. Latent heat flux, for instance, is used to estimate the consumptive water use of crops (McShane et al., 2017) which can then aid farmers in irrigation management. Generally, this study aimed to determine the partitioning of energy balance components in different biomes in Laguna, Philippines utilizing only remotely-sensed data which were then analyzed using the S-SEBI model. Specifically, this study endeavored to quantify the amount of heat flux received in Laguna; generate downscaled maps of net radiation, latent heat flux, sensible heat flux, and ground heat flux; and explain the comparison of the energy balance components among various biomes.

Materials and Methods

Study Area

Laguna was chosen to be the area of this study. Figure 2 shows the map of Laguna and the coordinates for the various biomes can be seen in Table 1.

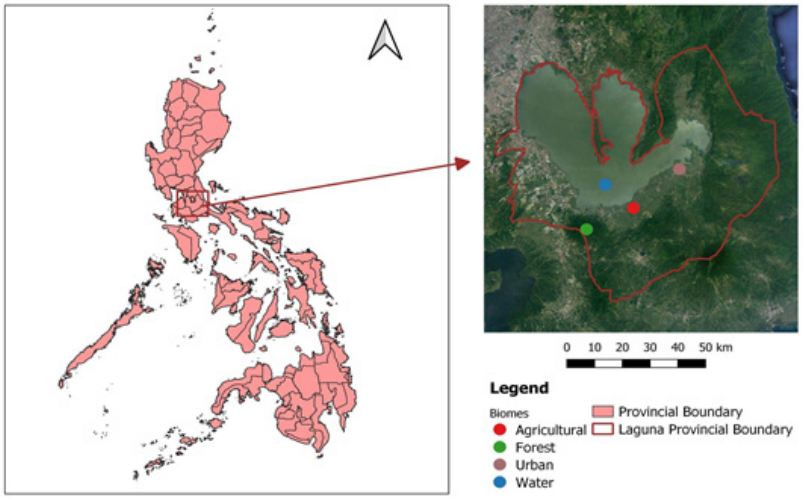

Table 1

Coordinates of Different Biomes

Biomes	Location	Coordinates
Water	Laguna de Bay	121.248120 °E, 14.243160 °N
Urban	Sta. Cruz	121.41256 °E, 14.28046 °N
Forest	Makiling Forest Reserve	121.206879 °E,14.136628 °N
Agricultural	Brgy. Bangyas, Calauan	121.310890 °E,14.187271 °N

Three Landsat 7 Enhanced Thematic Mapper Plus (ETM+) were used to determine the albedo and Normalized Difference Vegetation Index of Laguna. These data were chosen because they were clear and cloud-free. The information about the selected images can be seen in Table 1.

Table 2

Information of Landsat-7 ETM+ Images Used

Landsat-7 ETM+ Image	Date of Acquisition
LE07_116050_20011126	November 26, 2001
LE07_116050_20020403	April 3, 2002
LE07_116050_20030508	May 8, 2003

Raster calculations were made using Google Earth Engine. Albedo or surface reflectance for each image was computed using Equation 1 (Liang, 2000).

$$A=0.356r\_1+0.13r\_3+0.373r\_4+0.085\ \ r\_5+0.072r\_7-0.0018 \quad (1)$$

where A= albedo

r_(1) = reflectance of band 1
r_3 = reflectance of band 3
r_4 = reflectance of band 4
r_5 = reflectance of band 5
r_7 = reflectance of band 7

NDVI was then calculated using the reflected band and absorbed band as shown in Equation 2.

$$NDVI= (r\_4-r\_3)/(r\_4+r\_3) \quad (2)$$

where r_3 = reflectance of band 3 (red band)
r_4 = reflectance of band 4 (near infrared band)

In order to compute the surface energy balance parameters, other datasets were used. The general relationship of these parameters was given by Equation 3.

$$R_n=Q_L+Q_H+Q_G \quad (3)$$

where R_n = surface net radiation (W/m2)
Q_L = latent heat flux (W/m2)
Q_H = sensible heat flux (W/m2)
Q_G = ground heat flux (W/m2)

The surface net radiation can be derived using albedo and the components of net longwave radiation – upward longwave radiation and downward longwave radiation. It was calculated using the following equation:

$$R_n=(1-A)\ R_(g\ )+\ L_down-L_up \quad (4)$$

where R_n = surface net radiation (W/m2)
A = surface albedo
R_g = incoming global radiation (W/m2)
L_down = downward longwave radiation (W/m2)
L_up = upward longwave radiation (W/m2)

The incoming global radiation was obtained from the UPLBAgromet Station with the unit of cal/cm2 and then converted toW/m2. Table 3 shows the incoming global radiation. The other components were calculated using Equations 5, 6, and 7.

Table 3

Incoming Global Radiation at Different Periods

Date	Incoming Global Radiation (cal/cm^2)	Incoming Global Radiation (W/m^2)
November 26, 2001	259	125.571
April 3, 2002	663	321.2785
May 8, 2003	727	352.2918

The down welling longwave radiation was obtained using the air temperature obtained using Global Land Data Assimilation System 2.1 with approximately 25 km spatial resolution, vapor pressure from Terra Climate, with approximately 5 km spatial resolution and computed atmosphere emissivity. Equation 5 shows the calculation for atmosphere emissivity. ε^'=1.24

(e_a/T_a)^(1/7) (5).

where ε^' = atmosphere emissivity
e_a = vapor pressure (Pa)
T_a = air temperature (K)

Using the Stefan-Boltzman equation, the downward longwave radiation was obtained.

L_down=ε^' σT_a^4 (6)

where L_down = downward longwave radiation (W/m2)
ε^'= atmosphere emissivity
σ = Stefan-Boltzman constant (5.67 x 10^(-8))
T_a = air temperature (K)

The upward longwave radiation was also derived from the Stefan-Boltzman equation and was given by Equation 7.

L_up=εσT_0^4 (7)

where L_up= upward longwave radiation (W/m2)
ε = emissivity (1)
σ = Stefan-Boltzman constant (5.67 x 10^(-8) W/m2K4)
T_0 = surface temperature (K)

After computing the surface net radiation, the soil heat flux can be estimated using a relationship developed by Bastiaanssen (2000).

$$Q_G/R_n = T_0 (0.0038+0.0074A) \times (1-0.98NDVI^4) \quad (8)$$

where Q_G = ground heat flux (W/m2)
R_n = surface net radiation (W/m2)
T_0 = surface temperature (°C)

Latent heat flux and sensible heat flux were derived from the evaporative fraction and calculated using Equations 10 and 11.

$$Q_H=(1-\Lambda)(R_n-Q_G) \quad (10) \qquad Q_L=(1-\Lambda)(R_n-Q_G) \quad (11)$$

where Q_H = sensible heat flux (W/m2)
Q_L = latent heat flux (W/m2))
A = albedo
NDVI = normalized difference vegetation index

Using the S-SEBI model, albedo and surface temperature were plotted. The empirical coefficients for the evaporationcontrolled and radiation-controlled portions were determined. With the obtained constants, the evaporative fraction was computed.

$$\Lambda=(a_H+b_H \times A-T_0)/(a_H-a_LE+(b_H-b_LE)\times A) \quad (9)$$

where Λ = evaporative fraction
a_H,b_(H,) a_LE,b_LE = empirical coefficients
A = albedo
T_0 = surface temperature (K)
Λ= evaporative fraction
R_n= net radiation (W/m2)
Q_G = ground heat flux (W/m2)

Results and Discussion

Albedo

The fraction of the incoming solar energy reflected by Earth back to space is referred to as the planetary albedo. Figure 3 presents the map depicting the albedo in different biomes in the whole

province of Laguna during specific dates from 2001 to 2003. As can be seen in Table 4, albedo differs in every biome and the range of values is 0.046 to 0.363. The highest value of 0.363 was observed in agricultural land in November 2001. This might be due to the dry surface and the absence of crops because, at this period, rice was already harvested based on the cropping season in Laguna. Water body had the lowest albedo having an average value of 0.062. Moreover, the average albedo of the urban area was 0.151. In 2001, the albedo in the forest was high, but it declined to 0.125 and 0.128 in 2002 and 2003, respectively. This could be due to the phenological cycle of the trees. From 2001-2003, no pronounced changes in the albedo were observed for urban and water surfaces.

Figure 3

Albedo Map of Laguna during Different Periods

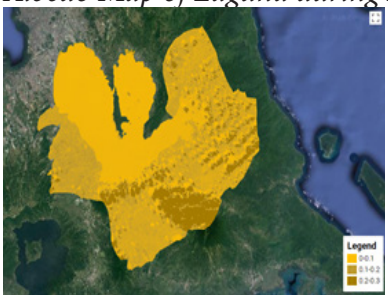

Albedo on November 26, 2001

Albedo on April 3, 2002

Albedo on May 8, 2003

Table 4

Albedo across Four Identified Biomes during Different Periods

Biomes	Albedo		
	2001	2002	2003
Water	0.046	0.051	0.089
Urban	0.144	0.15	0.158
Forest	0.314	0.125	0.128
Agricultural	0.363	0.124	0.2

According to Dobos (2005), the mean albedo of the earth was 0.36. Meanwhile, another study by Stephens et al. (2015) revealed that the mean reflectance value was 0.29. Albedo differs across various surfaces. Oceans, lakes, and forests reflect relatively small fractions of the incident sunlight and have low albedos. Snow, sea ice, and deserts reflect relatively large fractions of the incident sunlight and have large albedos. For any surface, the albedo depends on the spectral and angular distributions of the incident light, which in turn are governed by atmospheric composition and the direction of the beam of light from the sun (Coakley, 2003). The result of our study is in agreement with the other research. Briegleb et al. (1986, as cited in Coakley, 2003) stated that forest had an albedo of 0.12, while water body had an albedo of 0.07. Forest vegetation with a multilevel canopy has a low albedo, ranging from 0.05-0.2 because the incident radiation can penetrate deeply into the forest canopy where it bounces back and forth between the branches and leaves and gets trapped by the canopy (Dobos, 2005). Nutini et al. (2014) noted that desert areas have a higher albedo (0.6), while areas with lower temperatures such as lakes and rivers have lower albedo, approximately below 0.2. Rutan and Smith (2014) said diurnal variations of albedo are caused by the changes in solar zenith angle with the time of day and by changes in the atmosphere and surface through the day.

Normalized Difference Vegetation Index (NDVI)

Figure 4 shows the NDVI map in Laguna on three different dates. NDVI is higher in areas with dense vegetation and lowers in bare and water surfaces. The aforementioned statement is true to this study as forest obtained the highest NDVI among the four biomes

lowest values were observed in water as seen in Table 5. Urban and agricultural areas had an average of 0.423. It can be observed that the values for water and urban areas were consistent within the study period. The NDVI in forest and agricultural lands varies from year to year. In November 2001, the albedo in the forest was 0.251. This value increased to 0.847 and 0.874 in 2002 and 2003, respectively. This could be explained by the phenological cycle of the trees in the forest. The fluctuation of NDVI was pronounced in agricultural land. Its value in November 2001 was 0.101. However, it increased to 0.751 in April 2002 and decreased to 0.352 in May 2003. This high variation of NDVI in agricultural lands from time to time was mainly due to the cropping seasons and growth stages of the crop.

Figure 4

NDVI Map of Laguna during Different Periods

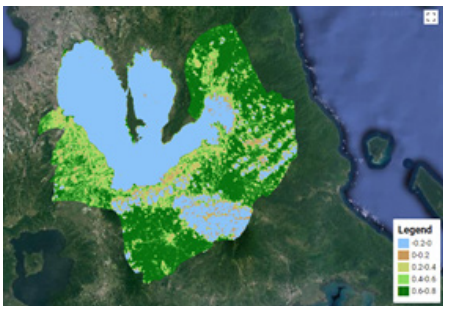

NDVI on November 26, 2001

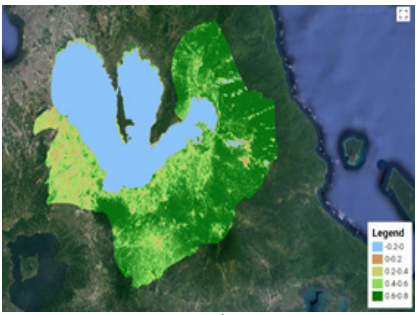

NDVI on April 3, 2002

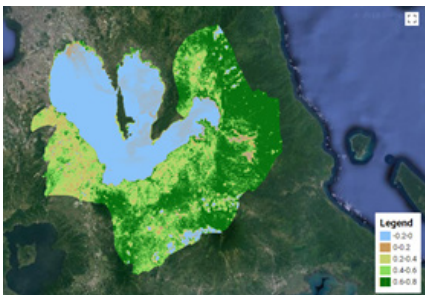

NDVI on May 8, 2003

Table 5

NDVI across Four Identified Biomes during Different Periods

Biomes	NDVI		
	2001	2002	2003
Water	-0.497	-0.514	-0.195
Urban	0.493	0.38	0.397
Forest	0.251	0.847	0.874
Agricultural	0.101	0.751	0.352

The two cropping seasons for rice can be seen in Figure 5. This explains the NDVI values for different periods in this study. In November, NDVI is low because the crops were already harvested. The peak value can be determined during the vegetative and early reproductive stages when the photosynthetic rate is high. For the dry season, the vegetative stage falls on April and the crop can be harvested in May.

Figure 5

Days of Year (DOY) of the Rice Area

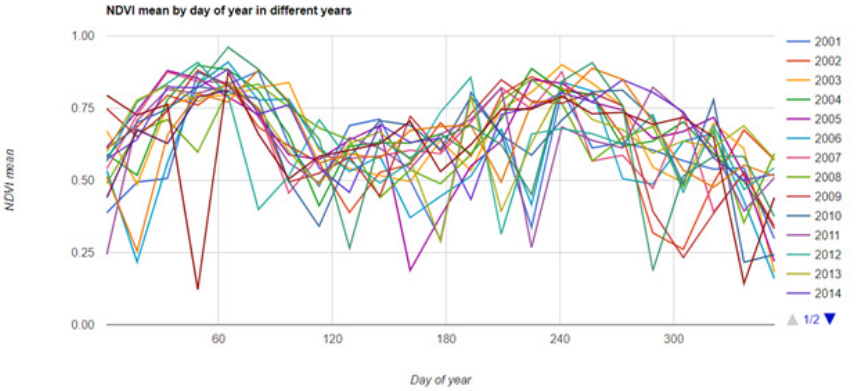

The result of this study is in consonance with the result of other studies. Defries and Townshend (1994) noted that forests had higher NDVI ranging from 0.3 to 0.8. Cultivated land and grassland had NDVI ranging from 0.2 to 0.4 and 0.2 to 0.3, respectively. They further observed that bare ground had a very low value of 0 to 0.1. Wright (2011) also noted that NDVI in dense vegetation canopy ranged from 0.3 to 0.8. Very low values of NDVI (0.1 and below) correspond to barren areas of rock, sand, or snow.

Holben (1986, as cited in Palanisamy & Gurugnanam, 2014) said that dense vegetation such as forests had an NDVI of 0.7, while

dry bare soil and water had very low NDVI with values of 0.025 and -0.257, respectively. Palanisamy and Gurugnanam (2014) further confirmed that dense forest had an NDVI value ranging from 0.45 to 0.7, while water bodies had a negative NDVI value (-0.06 to -0.35). Moreover, shrub and grassland had an NDVI value ranging from 0.078 to o.15, while barren areas and rock surfaces had an NDVI ranging from -0.35 to 0.078 (Palanisamy & Gurugnanam, 2014). Makiling forest reserve contained at least 225 families and 2,038 species of vascular plants (Combalicer et al., 2011). The entire forest reserve constantly marked high NDVI values ranging from 0.52 to 0.89. Combalicer et al. (2011) indicated the NDVI values, such as low values for lightly vegetated areas (0.1–0.2), moderate values for shrub and grassland areas (0.2–0.3), and higher values (0.4–0.7) for dense vegetation areas. Meanwhile, the negative values are represented by non-vegetative structures like water , clouds, and shadows (Combalicer et al., 2011).

Radiation

Upward and downward longwave radiations are components to estimate surface net radiation. The obtained maps for different periods can be viewed in Figures 6 and 7.

Figure 6

Upward Longwave Radiation Map of Laguna during Different Periods

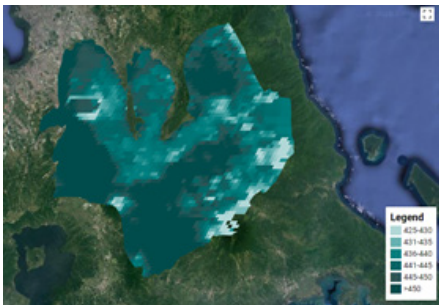

Upward Longwave Radiation on November 25, 2001

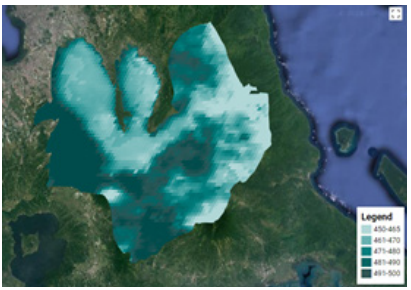

Upward Longwave Radiation on April 7, 2002

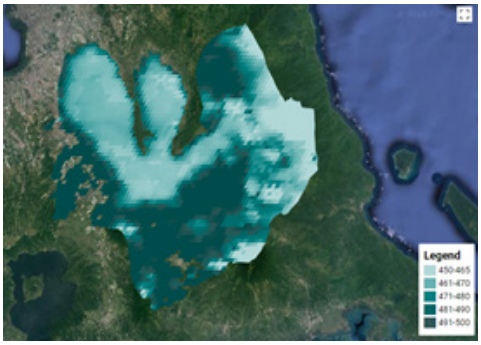

Upward Longwave Radiation on May 1, 2003

Figure 7

Downward Longwave Radiation Map of Laguna during Different Periods

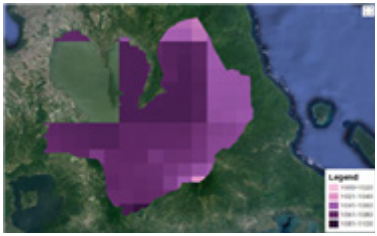

Downward Longwave Radiation on November 26, 2001

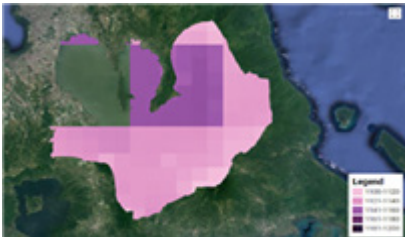

Downward Longwave Radiation on April 3, 2002

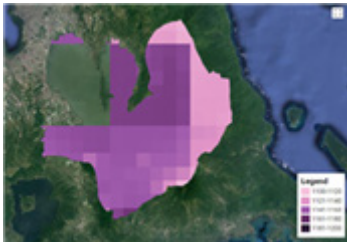

Downward Longwave Radiation on May 8, 2003

Figure 8 shows the net radiation maps of Laguna during different times. Net radiation was the dominant surface energy balance component, and its partitioning as latent heat, sensible heat, and soil heat fluxes depend on field surface and atmospheric conditions. Net radiation was high in water and forests due to the low albedo and high altitude of the forest. Santos et al. (2011) supported the idea that Rn values are higher in forested areas because they have lower albedo and reflect less shortwave radiation when compared to deforested areas like pasture. Forest, being darker, reflects less

energy and has the vertical structure of more than 30 meters on average, which pacifies the absorption of solar rays that penetrate the forest canopy and are absorbed in the inferior layers.

Urban, though low in albedo, has a slightly low net radiation that may be attributed to its atmospheric condition. Schönwiese (1994, as cited in Martinez & Ostos, 2004) summarizedthe alterations of climates due to urbanization, and one of these is the decrease in solar radiation due to urban atmospheric contamination. The lowest net radiation, on average, was observed in an agricultural area that has a high albedo.

Figure 8

Net Radiation Map of Laguna during Different Periods

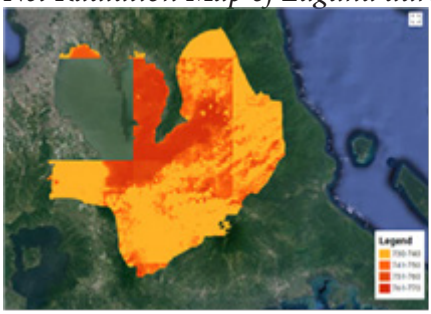

Net Radiation on November 26, 2001

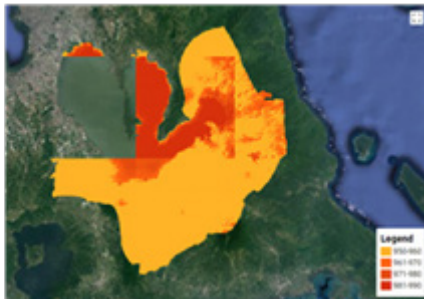

Net Radiation on April 3, 2002

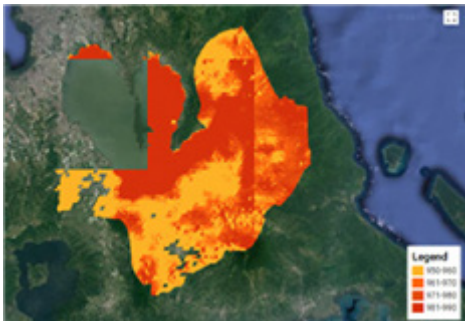

Net Radiation on May 8, 2003

Table 6

Net Radiation across Four Identified Biomes during Different Periods

Biomes	Net Radiation (W/m^2)			
	2001	2002	2003	Average
Water	769.496	976.944	1,023.14	923.1933
Urban	741.76	937.824	959.848	879.811
Forest	723.712	952.872	997.762	891.4489
Agricultural	691.736	921.981	957.91	857.209

Soil Heat Flux

In terms of soil heat flux, the urban area obtained the highest average value of 170.088 W/m2 followed by the agricultural area with 121.812 W/m2. Water and forest have had very low soil heat flux with values of 96.404 W/m2 and 66.775 W/m2, respectively. The variability of soil heat flux across four biomes was highest in urban areas (57-70 W/m2), followed by agricultural areas (22-55 W/ m2) and water (18-50 W/m2). The least variation of soil heat flux was observed in forests (2-44 W/m2).

Soil heat flux was higher in surfaces with minimal water content and intense surface heating. This was the reason why soil heat flux in urban areas was high. Water bodies and forests have had low soil heat flux due to minimal surface heating, as attributed to high moisture content and attenuation of light to the forest floor.

Figure 9

Soil Heat Flux Map of Laguna during Different Periods

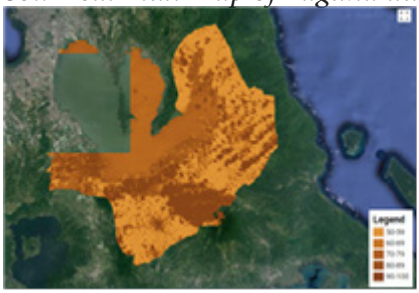

Soil Heat Flux on November 26, 2001

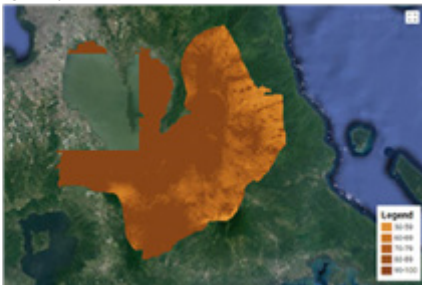

Soil Heat Flux on April 3, 2002

Soil Heat Flux on May 8, 2003

Table 7

Soil Heat Flux across Four Identified Biomes during Different Periods

Biomes	Ground Heat Flux (W/m^2)			
	2001	2002	2003	Average
Water	69.137	101.047	119.027	96.404
Urban	212.203	142.282	155.779	170.088
Forest	95.948	53.087	51.29	66.775
Agricultural	125.208	92.269	147.959	121.812

Table 8

Empirical Coefficients for Evaporative Fraction Calculation

Empirical Coefficient	November 26, 2001	April 3, 2002	May 8, 2003
a_H	36.061	39.855	48.349
b_H	-19.719	-6.3415	-34.788
a_{LE}	18.696	39.307	16.243
b_{LE}	26.545	18.781	58.048

Table 9 shows the obtained values for sensible heat flux. The urban area had the highest average sensible heat followed by the agricultural area and water bodies. The lowest observed was in forests, with an average value of 94 W/m2. From 2001 to 2003, the highest variation in sensible heat was observed in an agricultural area (74 to 226 W/m2), followed by water bodies (54 to 190 W/m2). Variation of sensible heat in forests and in urban was minimal, with variation values ranging from 4 to 45 W/m2 and 2 to 57 W/m2, respectively. Sensible heat flux, just like the other components of surface energy balance, is governed by the amount of water on a given surface. In urban areas, characterized by dry surfaces, sensible

heat flux is high. In forests, sensible heat is minimal since it has a relatively high amount of water on the soil surface and in the canopy itself.

Figure 10

Sensible Heat Flux Map of Laguna during Different Periods

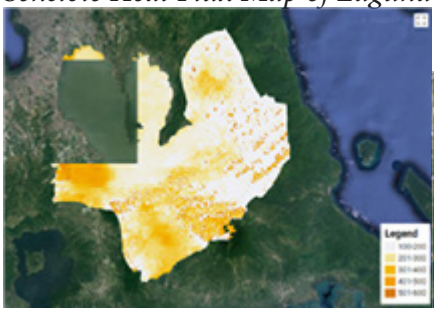

Sensible Heat Flux on November 26, 2001

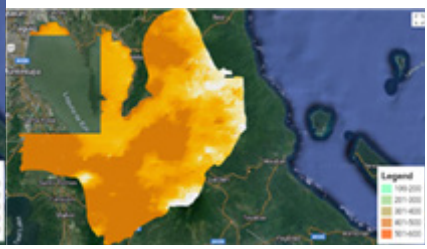

Sensible Heat Flux on April 3, 2002

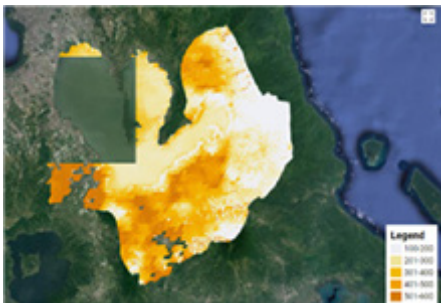

Sensible Heat Flux on May 8, 2003

Table 9

Sensible Heat Flux across Four Identified Biomes during Different Periods

Biomes	Sensible Heat Flux (W/m^2)			
	2001	2002	2003	Average
Water	120.792	310.435	174.813	202.013
Urban	314.939	316.418	371.362	334.240
Forest	123.00	82.508	78.993	94.834
Agricultural	183.894	335.009	109.139	209.347

Latent Heat Flux

Across four biomes, the values of latent heat flux also varied as observed in Figure 11. Table 10 shows the latent heat flux values

per biome. Forest had the highest amount of 729 W/m2, followed by water bodies with 624 W/m2 and agricultural land with 526 W/m2. The lowest latent heat flux of 375 W/m2 was determined in urban areas. The variations in the forest, agricultural, and urban were 50 to 362 W/m2, 111 to 317 W/m2, and 47 to 265 W m2, respectively. The lowest variation of latent heat was observed in the water bodies equal to 14 to 164 W/m2. Latent heat flux was high on wet surfaces and in densely vegetated areas. This was because latent heat flux is generally associated with evapotranspiration. With this, forest and water bodies, having high evapotranspiration, have had high latent heat flux.

Figure 11

Latent Heat Flux Map of Laguna during Different Periods

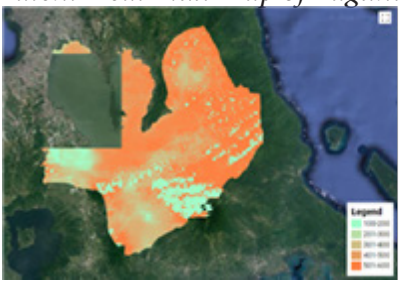

Latent Heat Flux on November 26, 2001

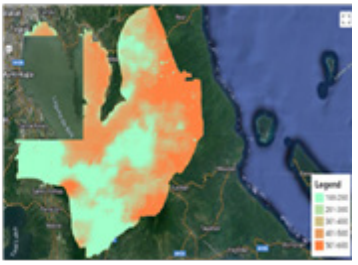

Latent Heat Flux on April 3, 2002

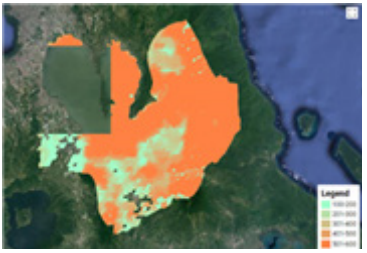

Latent Heat Flux on May 8, 2003

Table 10

Latent Heat Flux across Four Identified Biomes during Different Periods

Biomes	Latent Heat Flux (W/m^2)		
	2001	**2002**	**2003**
Water	579.567	565.462	729.294
Urban	214.618	479.123	432.707
Forest	505.01	817.277	867.48
Agricultural	383.422	494.703	700.813

Table 11 summarizes the average values of the surface energybalance components. The partitioning of net radiation in various biomes was shown in Figure 12. It can be observed that for all the biomes, latent heat flux dominated. On the other hand, the least component was soil heat flux.

In water, the dominant partition of the net radiation was a latent heat flux of approximately 658 W/m2, with a minimal sensible and ground heat flux (Zahira et al., 2009). This agrees with the result of this study. A study conducted by Martinez and Ostos (2004) found that urban area surrounded by vegetation had a high latent heat ranging from 120 to 320 W/m2, while its sensible heat ranged from 46 to 50 W/m2. In highly urbanized areas closely packed with massive buildings and with the relative absence of green evaporating areas, sensible heat is the dominant partition of the net radiation. The value ranged from 1.53 to 3.40 MJ/m2. For latent heat flux in these areas, the amount ranged from 0.37 to 0.39 MJ m2 (Miao et al., 2012; Oke et al., 1999). In this study, it was observed that latent heat flux in urban areas was quite greater than the sensible heat flux. The reason might be due to the presence of vegetation and a small water body within the vicinity.

Zahira et al. (2009) identified the ranges of latent heat flux, sensible heat flux, and soil heat flux for forest as 308 to 394 W/ m2, 164 to 222 W/m2, and 92 to 105 W/m2, respectively. Jiang et al. (2014) noted that latent heat in forests is higher compared to cropland and urban area.

In cropland, surface energy partitioning greatly depends on irrigation , and latent heat is dominant, corresponding with a decrease in sensible heat. In the absence of irrigation, sensible heat is the prevailing surface energy partition, while latent heat is only about half the amount of sensible heat (Lu & Kueppers 2012).

Table 11

Average Values of Surface Energy Balance Components across Different Biomes

Biomes	Surface Energy Balance Components			
	R_n (W/m²)	Q_G (W/m²)	Q_H (W/m²)	Q_L (W/m²)
Water	923.19	96.40	202.01	624.77
Urban	879.81	170.09	334.24	375.48
Forest	891.45	66.78	94.83	729.92
Agricultural	857.21	121.81	209.35	526.31

Figure 12

Partitioning of the Net Radiation across Different Biomes

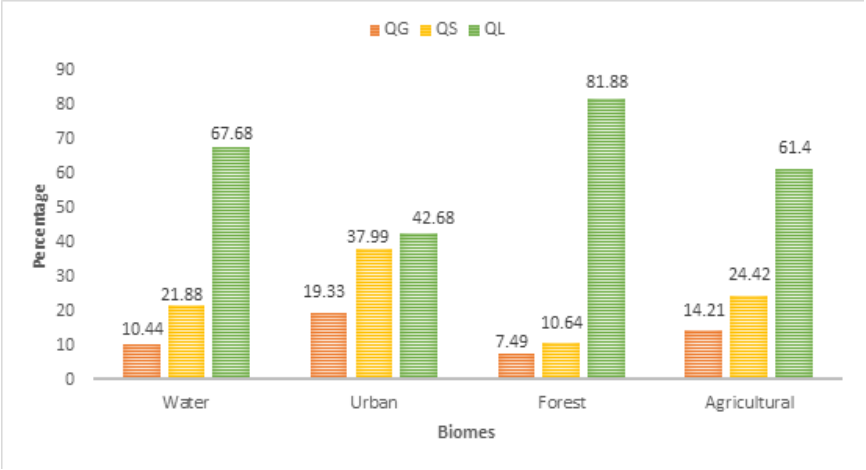

Summary and Conclusion

Surface energy balance components and partitioning greatly depend on surface covers, moisture, temperature, wind, and other micrometeorological parameters. Net radiation received by a certain surface is greatly influenced by its albedo. Meanwhile, the variation of soil heat flux, latent heat flux, and sensible heat flux in every ecosystem can be attributed to the availability or abundance of water and vegetation. Parallel to that, surfaces that are abundant in water and vegetation like forests have high latent heat flux, minimal sensible heat flux, and almost negligible soil heat flux. Dry surfaces, in contrast, are characterized by high sensible heat flux with a considerable amount of soil heat flux and minimal latent heat flux.

In this study, net radiation, sensible heat flux, latent heat flux, and soil heat flux of different biomes in Laguna were estimated using the S-SEBI Method. It was found that soil heat flux was the least partitioned across all the biomes. Latent heat flux is dominated followed by sensible heat flux. Comparing the components for each biome, ground heat flux and sensible heat flux were high in urban and agricultural areas. Meanwhile, latent heat flux was high in forest and water bodies.

Based on the amount of albedo, water received the highest amount of net radiation, while agricultural areas received the least.

Also, due to high altitude and low albedo, net radiation in the forest was considerably high. Generally, the result obtained in this study is comparable to the findings of the existing studies. The method employed in this study, therefore, is costefficient and reliable in partitioning the surface energy balance components that fluctuate dynamically in each ecosystem as a consequence of surface covers, moisture, temperature, wind, and other micrometeorological parameters.

Recommendation

In order to improve this study, it is recommended to use Landsat 8 data that give the latest images. Also, for accurate values, it is highly encouraged that more than one station should be used to obtain the incoming solar radiation if this method will be replicated in another area or use the Hargreaves-Samani equation. Instruments for direct measurement of these parameters are necessary for ground validation.

References

Arulbalaji, P., & Gurugnanam, B. (2014). *Evaluating the normalized difference vegetation index using Landsat Data by ENVI in Salem District, Tamilnadu, India*. ResearchGate. https://www.researchgate.net/publication/272182220_evaluating_the_normalized_difference_vegetation_index_using_landsat_data_by_envi_in_salem_district_tamilnadu_india

Bastiaanssen, W. G. M. (2000). SEBAL-based sensible and latent heat fluxes in the irrigated Gediz Basin, Turkey. *Journal of Hydrology, 229*, 87–100.

Borowik, T., Pettorelli, N., Sönnichsen, L., & Jędrzejewska, B. (2013). Normalized difference Vegetation index (NDVI) as a predictor of forage availability for ungulates in forest and field habitats. *Eur J Wildl Res, 59*, 675–682. doi: 10.1007/s10344-013-0720-0

Coakley, G. A. (2003). *Reflectance and albedo surface*. GiorgiaTech. http://www.curry.eas.gatech.edu/Courses/6140/ency/Chapter9/Ency_Atmos/Reflectance_Albedo_Surface.pdf

Defries, R. S., & Townshend, J. R. G. (1994). NDVI-derived land cover classifications at a global scale. *International Journal of Remote Sensing, 15*(17), 3567-3586. doi:10.1080/01431169408954345

Dobos, E. (2005). *Albedo*. ResearchGate .https://www.researchgate.net publication/242547003_Albedo

Google Earth Engine. (2018). FAQ. https://earthengine.google.com/faq/

He,T., Liang, S., Song, D. X. (2014). Analysis of global land surface albedo climatology and spatial-temporal variation during 1981–2010 from multiple satellite products, J. Geophys. *Res. Atmos., 119*(10), 281–10, 298. doi:

Jiang , Z., Huete, A. R., Chen, J., Chen, Y., Li, J., Yan, G., Zhang, X. (2006). Analysis of NDVI and scaled difference vegetation index retrievals of vegetation fraction. *Remote Sensing of Environment 101*, 366–378. doi:10.1016/j.rse.2006.01.003

Jiang, Q., Tang, C., Ma, E., Yuan, Y., Zhang, W. (2014). Variations of near surface energy balance caused by land cover changes in the semiarid grassland area of China. *Advances in Meteorology*. http://dx.doi.org/10.1155/2014/894147

Lantican, R. M. (2001). The science and practice of crop production. : SEAMEO SEARCA and UPLB.

Liang, S. (2000). Narrowband to broadband conversions of land surface albedo I algorithms. *Remote Sensing of Environment, 76*, 213-238.

Liou, Y., Kar, S. K. (2014). Evaporation estimation with remote sensing and various surface energy balance algorithms: A review. *Energies,* 7(5), 2821-2849. doi:10.3390/en7052821

Laguna Lake Development Authority. (2018). *Laguna de Bay*. http://llda.gov.ph/laguna-de-bay/

Lu, Y., & Kueppers. L. M. (2012). Surface energy partitioning over four dominant vegetation types across the United States in a coupled regional climate model (Weather research and forecasting model 3–Community land model 3.5). *J. Geophys. Res., 117*, D06111. doi:10.1029/2011JD016991

Martínez, A. T., & Ostos, E. J. (2005). *Surface energy balance measurements in the México City region: A review.* http://www.scielo.org.mx/scielo.php?script=sci_arttext&pid=S0187-62362005000100001

McShane, R. R., Driscoll, K. P., Sando, R. (2017). A review of surface energy balance models for estimating actual evapotranspiration with remote sensing at high spatiotemporal resolution over large extents. U.S. *Geological Survey Scientific Investigations Report,* 2017–5087, 19 p. https://doi.org/10.3133/sir20175087

Miao, S. G., Dou, J. X., Chen, F. (2012). Analysis of observations on the urban surface energy balance in Beijing. *Sci China Earth Sci, 55*, 1881-1890. DOI: 10.1007/s11430-012-4411-6 arid rangeland

Nutini, F., Boschetti, M., Candiani, G., Bocchi, S., & Brivio, P. A. (2014). Evaporative fraction as an indicator of moisture condition and water stress status in semi-arid rangeland ecosystems. *Remote Sens.*, *6*, 6300-6323. DOI:10.3390/rs6076300

PhilGIS. (2018). *Laguna*. http://philgis.org/province-page/laguna

Rutan, D. A., Smith, G. L. (2014). Diurnal variations of albedo retrieved from earth radiation budget experiment measurements. *Journal of Applied Meteorology and Climatology, 53* (2), 2747-2760. doi: 10.1175 JAMC-D-13-0119.1.

Saludes, R. B. (2018). Surface energy balance [Powerpoint slides].

Santos, C. A., Nascimento, R. L., Rao, T. V. (2011). *Net radiation estimation under pasture and forest in Rondônia, Brazil, with TM Landsat5 images*. https://www.google.com.ph/search?q=Net+radiation+estimation+under+pasture+and+forest+in+Rond%C3%B4nia%2C+Brazil%2C+with+TM+Landsat+5+images&rlz=1C1RLNS_enPH765PH765&oq=Net+radiation+estimation+under+pasture+and+forest+in+Rond%C3%B4nia%2C+Brazil%2C+with+TM+Landsat+5+images&aqs=chrome..69i57j69i61.1058j0j9&sourceid=chrome&ie=UTF-8

Stephens, G. L., O'Brien, D., Webster, P. J., Pilewski, P., Kato, S., & Li, J. -l . (2015). The albedo of earth. Rev. *Geophys.*, 53. doi:10.1002/2014RG000449

Verhulst, N., & Govaerts, B. (2010). The normalized difference vegetation index (NDVI) GreenSeekerTM handheld sensor: Toward the integrated evaluation of crop management. *Part A: Concepts and case studies.* CIMMYT.

Xin, F. Y., Chen, F., Zhao, P., Barlage, M., Blanke, P., Chen, Y.L., Chen, B., & Wang, Y. J. (2018). Surface energy balance closure at ten sites over the Tibetan plateau. *Agricultural and Forest Meteorology, 259*, 317–328.https://doi.org/10.1016/j.agrformet.2018.05.007

Yengoh, G. T., Dent, D., Olsson, L., Tengberg, A. E., & Tucker, C. J. (2014). *The use of the Normalized Difference Vegetation Index (NDVI) to assess land degradation at multiple scales: A review of the current status, future trends, and practical considerations.* Lund University Center for Sustainability Studies (LUCSUS), and The Scientific and Technical Advisory Panel of the Global Environment Facility (STAP/GEF).

Zahira, S., Abderrahmane H., Mederbal, K., & Frederic, D. (2009). Mapping latent heat flux in the western forest covered regions of Algeria using remote sensing data and a spatialized model. *Remote Sensing , 1*, 795-817. doi:10.3390/rs1040795

Zaitunah, A., Ahmad, A. G., & Safitri, R. A. (2018). Normalized difference vegetation index (NDVI) analysis for land cover types using landsat 8 oli in besitang watershed, Indonesia. *Earth and Environmental Science, 126,* 012112. doi:10.1088/1755-1315/126/1/012112